

Chemo-Rheological Behavior of Aqueous Titanium Carbide Suspension and Evaluation of the Gelcasted Green Body Properties

Hamze Foratirad^{a*}, Hamid Reza Baharvandi^b, Mohammad Ghanadi Maragheh^a

^a Nuclear Fuel Cycle Research School, Nuclear Science and Technology Research Institute, Tehran, Tehran Province, Iran

^b Department of Materials Science and Engineering, Malek-Ashtar University of Technology – MUT, Tehran, Tehran Province, Iran

Received: May 30, 2016; Revised: October 17, 2016; Accepted: November 21, 2016

Gel-casting is an advanced colloidal processing method for fabricating ceramic green parts. In this project acrylamide-based monomers were used as a gelcasting system. The effects of tetramethylammonium hydroxide and polyethylenimine dispersants on the premix solution containing titanium carbide powder have been studied via observation of the zeta potential and rheological behavior. The effect of various parameters on the gelation time and viscosity of solution and flexural strength and the shrinkage rate of titanium carbide green body were investigated. The results presented that the order of dispersion capacity of the tetramethylammonium hydroxide dispersant was better than the polyethylenimine dispersants. The results showed that the gelation time decreased and viscosity increased with increasing the monomer content, solid loading, initiator amount and temperature. The highest bending strength (39 MPa) was obtained for the samples containing 25 wt.% monomer content and 50% solid loading.

Keywords: Gel-casting, Titanium Carbide, Rheological Behavior

1. Introduction

Titanium carbide with the excellent mechanical and thermal properties at elevated temperature has been widely used for high temperature applications¹⁻⁶. It has high modulus, hardness and strength and excellent wear and oxidation resistance. Also, it has low coefficient of thermal expansion and high thermal conductivity. However, it is difficult to produce ceramic bodies with complex shapes and accurate dimensions by the conventional forming techniques. For many of these applications, the gelcasting process is extensively used⁷⁻⁹.

Gelcasting is a near-net-shape ceramic forming method with high green body strength, which was first developed at Oak Ridge National Laboratory by Omatete and Janney during the 1990s¹⁰. In gelcasting, a concentrated ceramic slurry is created by mixing a ceramic powder and a monomer solution. After this, the ceramic suspension is poured into a mold to get the desired shape, then removed from the mold and finally dried. The principle of the gelcasting process is based on the in-situ polymerization of an organic monomer solution which forms a 3-dimensional macromolecular network that holds powders together¹⁰. In order to produce ceramic products with good performance, dimensional stability and high green strength, a fluid ceramic slurry with low viscosity and with as high solid loading as possible is required. High solid loading increases the viscosity and on the other side, reduces the shrinkage. The optimal conditions can be obtained if an appropriate dispersant concentration is used¹¹.

The most important process step in slurry processing for production of ceramics which can significantly improve the final properties of bodies, is obtaining a homogenous structure with low shrinkage rate and high green strength. It is an imperative to have slurry with good dispersion and a desirable rheological behavior, because the quality of dispersion controls the casting behavior and the resulting green-body properties. However, the parameters which can influence the physical properties of the ceramic green body (e.g., gelation time, shrinkage, and strength of green body) are monomer composition, monomer content, monomers ratio, the amounts of initiator and catalyst additives, solid loading, temperature and dispersant.

Although a number of studies have investigated the preparation of TiC ceramics by gelcasting^{12,13}, few investigations have been carried out into the influences of the gelcasting parameters on the rheological behavior and properties of the green body. In this paper, the gelcasting of titanium carbide is studied and optimized in terms of dispersant type, dispersant concentration, monomer content, monomer ratio, initiator and catalyst amounts, solid loading and temperature.

2. Experimental

The starting ceramic powder used in this experiment with an average particle size of 3-5 μm was a commercial high-purity titanium carbide (Pacific Particulate Materials (PPM) Ltd, Canada) with the specific surface area 2.2 m^2/g and 0.11% retained free carbon. Aqueous gelcasting was processed using acrylamide (AM, $\text{C}_2\text{H}_3\text{CONH}_2$, Sigma-

* e-mail: hforatirad@aeoi.org.ir

Aldrich) as a monomer, N,N'-methylenebisacrylamide (MBAM, $(C_2H_3CONH_2)_2CH_2$, Sigma-Aldrich) as a cross-linker, N,N,N',N'-tetramethylethylenediamine (TEMED, $(CH_3)_2NCH_2CH_2N(CH_3)_2$) as a catalyst and ammonium persulfate [APS, $(NH_4)_2S_2O_8$] as an initiator (both from Sigma-Aldrich Co., US). Figure 1 shows the molecular structures of monomer system components. In order to compare the various dispersants, Tetramethylammonium hydroxide (TMAH, $C_4H_{13}NO$, Merck Co.) and Polyethylene imine (PEI, $(C_2H_5N)_n$, Merck Co.) were used as the dispersants. The quantity of dispersants applied with respect to the previous studies¹⁴, were selected at the 0.4 and 2wt% of the ceramic powder, respectively. The gelcasting flow chart presented in Figure 2 shows the process of producing the final products from the titanium carbide powder. The slurries were degassed for 10 min after casting in the mold. The slurry was degassed for another 10 min when the initiator and catalyst were added. After the monomers had polymerized, the green bodies were demolded. After gelcasting, the samples were dried in a commercial oven, at 60 °C with relative humidity of 70% for 60 h.

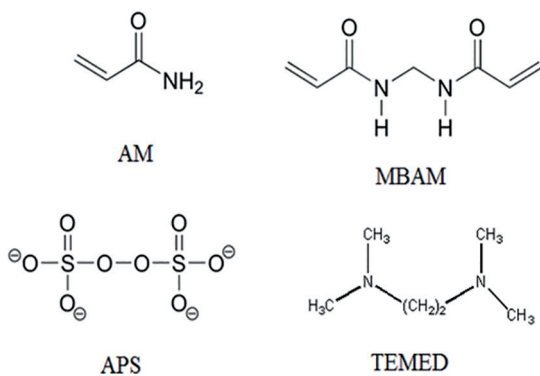


Figure 1: The molecular structures of monomer system components.

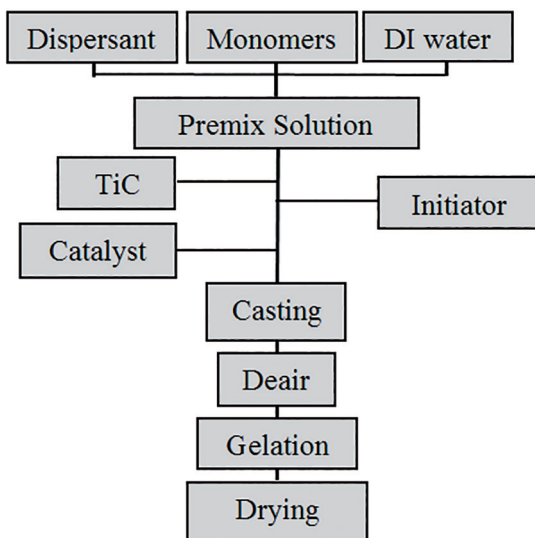


Figure 2: Flow chart of gelcasting process.

At first, the influence of various dispersants and solids loading on the zeta potential and rheological behavior of TiC suspension was investigated. And then, various monomer pre-mix solutions, with different monomer contents, monomers ratio and initiator contents were prepared and the gelation behavior of these systems in the presence or absence of ceramic powder and at different temperatures was investigated and compared with each other. Gelation was initiated immediately after adding predetermined amounts of initiator and accelerator.

The surface chemical properties of as-received powders was determined using by FTIR spectroscopy (Spectrum one, Perkin-Elmer, Wellesley, MA) after mixing with KBr powder. Z-potential measurements were performed by an acoustic and electroacoustic spectrometer (DT-1200, Dispersion Technology Inc., Bedford Hills, NY). The zeta potentials were recorded as a function of the pH of the suspension. The titration was automatically performed by means of a built-in autotitrator using 0.1M HCl and 1M NaOH solutions. The shear viscosity and the time dependency of pre-mix solutions and viscosities during gelation were measured by a Visco 88 viscometer with a concentric-cylinder having a diameter of 30 mm. Steady state shear flow curves were measured in a shear rate range between 0.03 and 200 S^{-1} . A digital thermometer (i.e. pH-mV-temperature meter with an accuracy of 0.1 °C, Lutron TM-905, Taiwan), was used to measure the temperature of pre-mix solutions and suspensions during the progress of gelation. The bending strength of the dried samples were determined by a three-point flexure test in accordance with ASTM C1161 with Universal Testing Machine (ZWICK, Z050) at 0.5 mm/min loading rate. The fracture surfaces morphologies of the fabricated porous ceramics were investigated by scanning electron microscopy (SEM V18 ZEISS).

3. Result and discussion

The TiC powder surface layer composition was determined by FT-IR spectroscopies analyze. Figure 3 shows the FT-IR spectrum of the as-received TiC powder. The peak centered at 466 cm^{-1} can be attributed to the Ti-C vibration. The band at 611 cm^{-1} and 1450 cm^{-1} are due to titanium oxide and assigned to the lattice vibrations of TiO_2 . The peak centered at 1012 cm^{-1} can be attributed to characteristic O-O stretching vibration. The absorption band at 1639 cm^{-1} is due to the bending vibration of coordinated H_2O as well as Ti-OH. The absorption of hydroxyl groups was created the broad peaks at 3450 cm^{-1} . The FT-IR results indicated the presence of TiO_2 on the surface of the received powders. Therefore, it could be concluded that the surface properties of TiC powders were largely determined by the TiO_2 composition on their surface¹⁵.

Zeta potential of TiC powders in the absence of any dispersant in deionized water is shown in Figure 4. The

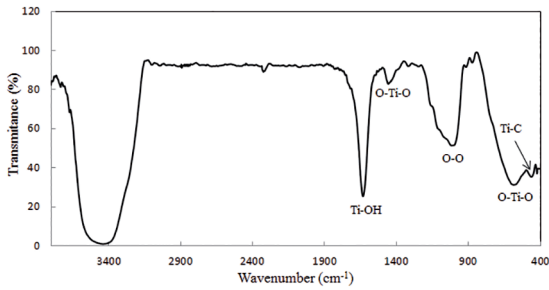


Figure 3: FT-IR spectra of as-received TiC powders in the wavenumber range of 4000–400 cm^{-1} .

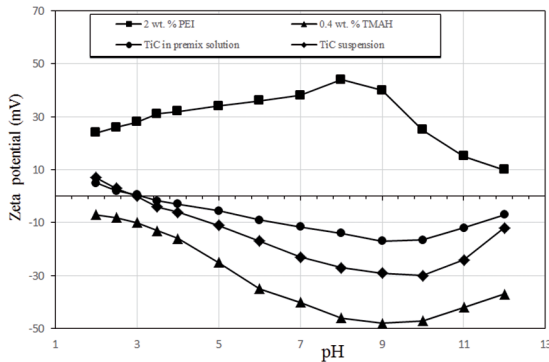


Figure 4: Zeta potential of TiC suspension without dispersant and TiC in the premix solution with and without dispersant.

isoelectric point (IEP) of TiC powders is at pH 3.1. The TiO_2 surface oxide in the presence of water easily hydrolysed to Ti-OH groups. When the pH is lower than the IEP, Ti-OH reacts with H^+ leaving Ti-OH_2^+ with positive zeta potentials. When the pH is higher than the IEP, Ti-OH reacts with OH^- , yielding Ti-O^- with negative zeta potentials¹⁶. Zeta potential of TiC powders in the presence of the monomer (premix solution), was decreased compared to TiC suspension without dispersant. It suggests that the uncharged monomer molecules screen the charge developed at the solid/liquid interface and decrease the stability of suspension¹⁷. TMAH dispersant dissociates to $(\text{CH}_3)_4\text{N}^+$ and OH^- in the presence of water¹⁸ and Hydroxyl group promotes the production Ti-O^- inducing more negative charge on the TiC surface. The IEP of TiC suspension disappeared with 2 wt. % PEI addition (Figure 4) and a highly positive surface charge was achieved at the low pH. PEI is a cationic polymer with repeating unit composed of the amine group and two carbon aliphatic CH_2CH_2 spacers. When an amino group is protonated, it will be attracted to the negatively charged Ti-O^- surfaces group. The protonation of the amine groups in PEI molecules and subsequent expansion of the polyions due to the mutual charge repulsion are responsible for highly positive zeta potential in the wide pH range (positive zeta potential with a value of 30 to 44 mV was obtained in the pH range 5 to 10). In the high pH range (pH > 10), PEI actually carries no charge and the polymers exist as free molecules

and thus zeta potential values decrease gradually. The results show that the TMAH and PEI dispersants can increase the stability of suspensions. However, the TMAH dispersant provides good dispersion compared with the PEI dispersant¹⁸.

Figure 5 shows the effect of dispersant concentrations on the viscosity of premix solutions containing 50 vol. % TiC, 20 wt. % monomers content (AM + MBAM) and the ratio AM/MBAM of 10, as a function of shear rate at the pH = 9. In any concentration, the flow curve deviates from a Newtonian behavior or shear thinning behavior. This behavior is characterized by the decrease in viscosity at increasing shear rates¹⁹. It is obvious that the viscosity of the slurry decreases with an increase in the dispersant dosage. It is worth mentioning that an optimum concentration of the dispersant is 0.4 wt. %. The viscosity of slurries increases suddenly as the concentration of the dispersant increases to 0.6 wt. %. Additional dispersant ions cause the compressive effect on the electrical double layer (EDL) and so, the thickness of the charge cloud on the surface of titanium carbide particles decreases, thereby decreasing the repulsive forces and suspension stability^{18,19}.

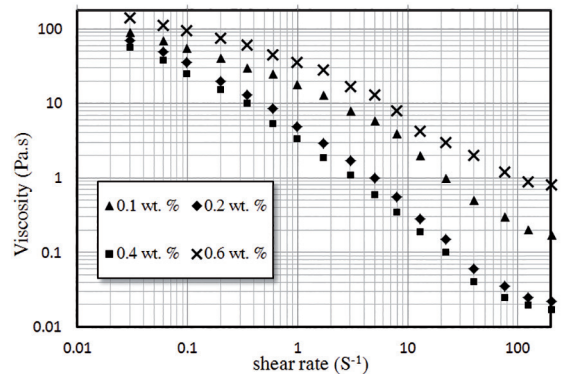


Figure 5: The effect of dispersant concentrations on the viscosity of premix solutions containing 50 vol. % TiC.

Figure 6 shows the rheological properties of the TiC suspensions vs. different solids loading at the 0.4 wt. % dispersant. It can be seen from the curves that the suspensions in all of the solid loading show shear thinning behavior and belong to pseudoplastic fluid. It also can be found from the curves that the viscosity of suspension increases with the solid loading again. In the solid loading below the 50 vol. %, suspension viscosities are lower than 1 Pa.s and to be enough to provide the required stability to the slurry. There is a substantial increase in the viscosity, when solid loading reaches 60 vol. %. The viscosity increases to > 1 Pa.s at shear rate of 75 s^{-1} , which is not suitable for the gelcasting process¹⁹.

Figure 7 shows the fracture surface of the resulted green body (20 wt. % monomers content, 50 vol. % solid loading and 0.4 wt. % dispersant) with a compact and homogeneous distribution appearance and a limited number of pores. As seen in the figure, the TiC powders have been almost uniformly

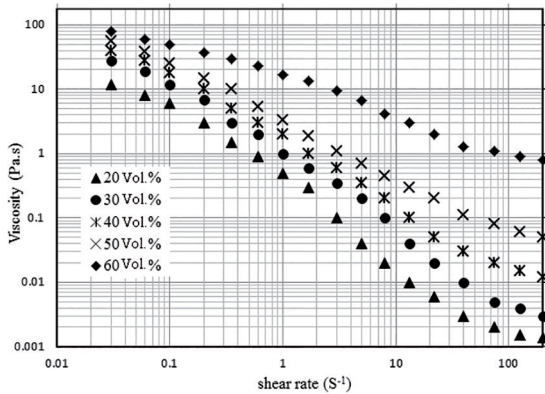


Figure 6: Variation of viscosity with the solid loading in the 0.4 wt. % TMAH dispersant at different shear rates.

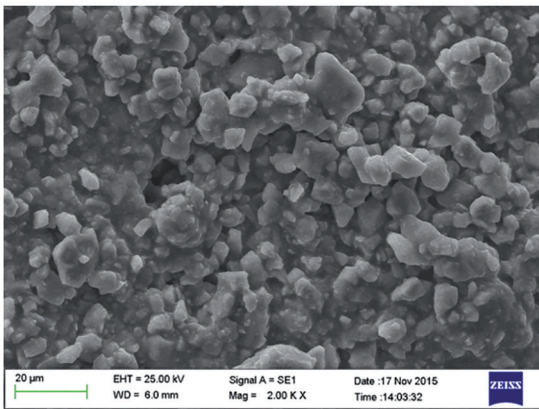


Figure 7: SEM micrograph of fracture surface of TiC green body gelcasted with 0.4 wt. % dispersant.

dispersed and also the grains are connected by 3D polymeric networks which are responsible for the strength of the green body. The limited number of the holes in the sample can also be caused by the air caption in the gelcasting process.

The idle time, t_{idle} , i.e. the time between the addition of the initiator and the catalyst and the beginning of polymerization that is equivalent to the time available for casting the slurry. Idle time is affected by several factors such as monomer concentration, monomer to cross-linker ratio, initiator concentration, amount of solid loading and solution temperature²⁰⁻²². Figures 8 and 9 show the changes in the t_{idle} and viscosity of the pre-mix solution as the function of monomer content, molar concentration of AM, molar concentration of MBAM, weight ratio initiator to monomers (AM+MBAM), volume fraction of TiC and temperature, respectively. As shown in Figure 8a, idle time decreases with the increase of monomer. Also, as seen in Figure 9a, viscosity increases relatively slow during a certain period and then increases rapidly with increasing monomer content. The higher the concentration of the monomer, the faster polymerization. It is due to an increase in the polymer chain length and formation of intermolecular crosslinking

through more crosslinking sites at intense concentrations of the polymer. Hence, the polymerization rate increases, which decreases the gelation time. In the low monomer content, the polymer chains are too distant from each other and to form intermolecular crosslinking readily²³.

Figs. 8b and 9b show the t_{idle} and the viscosity changes versus various concentrations of AM with constant other parameters. According to the diagram, the gelation time reduced and the viscosity increased with an increase in AM concentration as a germ of polymerization. The gelation of a polymer with high molecular weights will be faster than the polymers with lower molecular weights. The higher the amount of AM, the increased the polymer chain length and the average molecular weight of polymer chain. As the molecular weight increases, the probability for a polymer chain to form entanglements with the neighboring polymer chains increases and therefore the probability of polymerization reaction increases^{24,25}.

The role of MBAM concentration on gelation kinetic of solution and viscosity of pre-mix solution with constant AM and APS concentrations in 23 °C can be found from Figs. 8c and 9c. The results showed that the gelation time decreases and the viscosity increases with increasing MBAM concentration as a cross-linker. Polymer chains are often interconnected to form a nonlinear, branched, or crosslinked polymer. Branching is analogous to the extra arms growing out of a polymer chain; thus, the probability of the entangled, physical connections among the chains increases with the MBAM concentration increase²⁶.

Figs. 8d and 9d show the variation of the gelation time and viscosity of pre-mix solutions with respect to the amount of the initiator (APS) with constant AM and MBAM concentration at 23 °C. As seen in the figures, the reduction of the initiator concentration increases t_{idle} and decreases the viscosity. Polymerization is initiated by the generation of free radicals from persulfate, so that an increase in APS amount results in a decrease in t_{idle} . Dependence of gelation time and viscosity on the solid loading are shown in Figs. 8e and 9e. The solids loading of suspensions also has a crucial effect on the rheological behavior due to adsorption of charged dispersants. In the general, the viscosity of suspensions increases with increasing solids loading due to the reduction of the inter particle distance. By increasing solid loading, the present solution volume decreases and so the concentration of the monomers and cross-linkers around the particles increases. As a result, it becomes easier for the AM and MBAM in the slurry to copolymerize and so the idle time is reduced significantly. Indeed the ceramic powder has an accelerating effect in the polymerization process. The variation of the gelation time and viscosity with pre-mix solution temperature are shown in Figure 8f and 9f. The results show clearly that the gelation time is decreased when the temperature of pre-mix solutions is increased. Temperature has a direct effect on the rate of gel polymerization; the polymerization

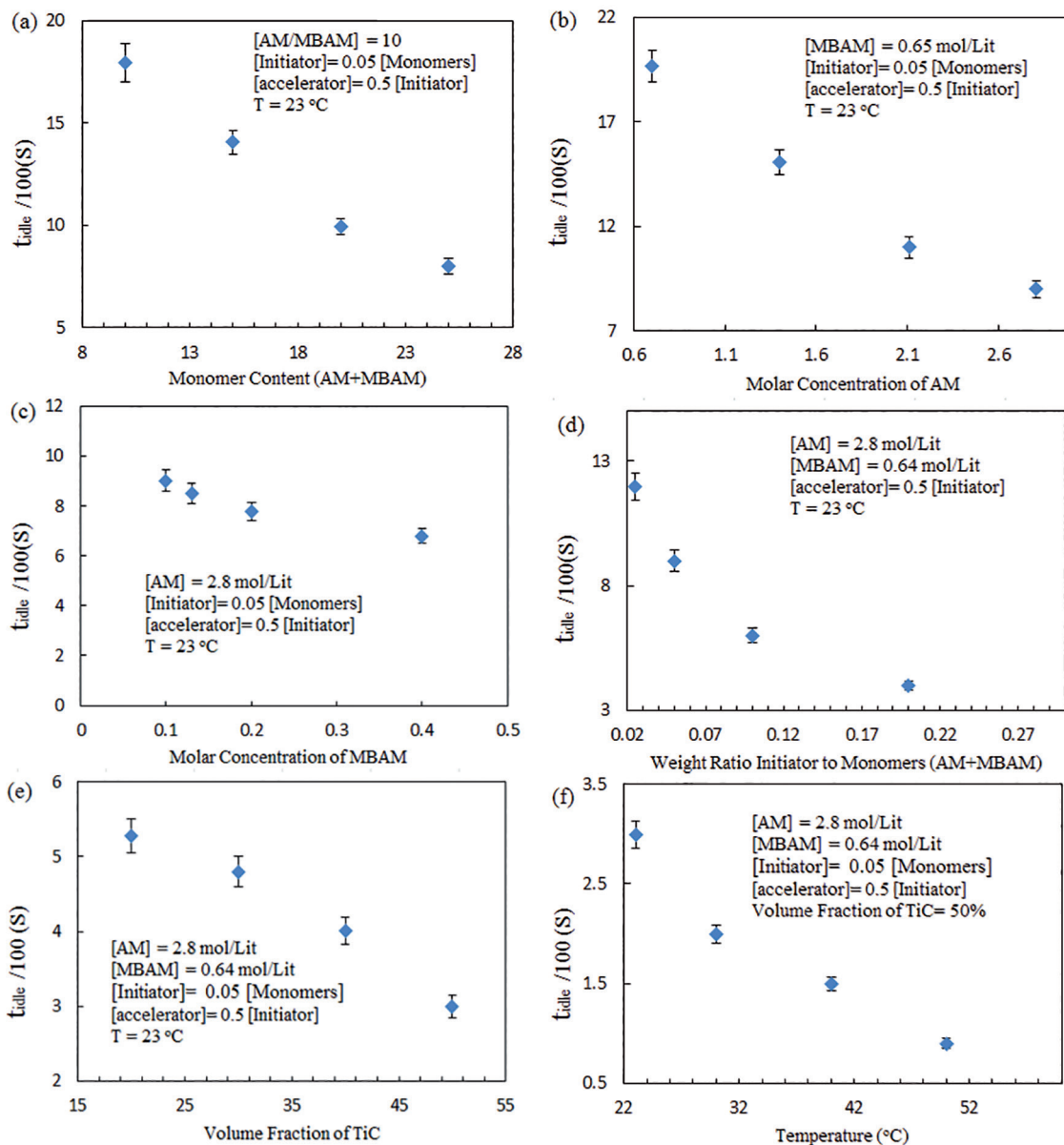


Figure 8: The changes in the t_{gel} of the pre-mix solution as the function of (a) monomer content, (b) molar concentration of AM, (c) molar concentration of MBAM, (d) weight ratio initiator to monomers (AM+MBAM), (e) volume fraction of TiC and (f) temperature.

reaction is also exothermic. Consequently, the generated heat quickens the reaction, considerably. Thus, gelation usually occurs very rapidly once polymerization begins.

The variation of bend strength of the green bodies as a function of monomers ratio and monomer content for 40 vol.% solid loading is presented in Figure 10. As seen in the figure, in different monomer contents, the flexural strength of green bodies shows similar trends with the monomers ratio change. At first, the flexural strength increases with the monomers ratio increase until it reaches a maximum value at 12.5 ratios, then decreases for higher monomers ratio. Crosslinking forms bridges between the chains and

dramatically increases molecular weight. Consequently, the physical and mechanical properties vary with the composition and extent of the crosslinking for a given polymer system. When the monomers ratio is low, the cross-linker is excessive and the three dimensional network structures of the cross-linked polymer are coarse so as to decrease the toughness of network structures and then the flexural strength of the green body decreases. On the other side, when the monomers ratio is too high, the three dimensional network structures are loose, thereby reducing the flexural strength of green body²⁷.

The monomers content and solid loading play an important role in determining the strength of the green gelcast bodies.

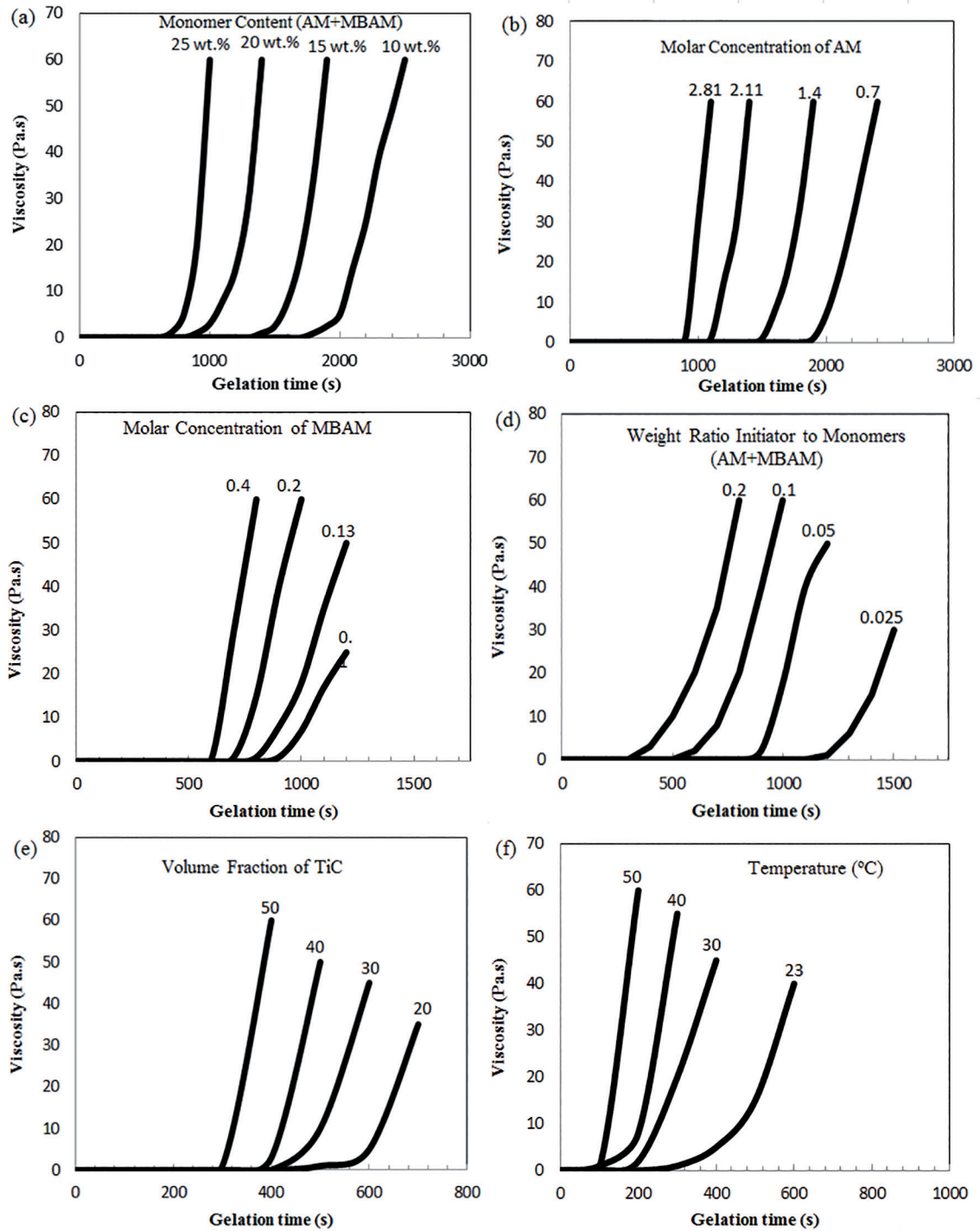


Figure 9: The changes in the viscosity of the pre-mix solution as the function of (a) monomer content, (b) molar concentration of AM, (c) molar concentration of MBAM, (d) weight ratio initiator to monomers (AM+MBAM), (e) volume fraction of TiC and (f) temperature.

Figure 11 shows the influences of monomer content and solid loading on the bending strength of the green body. The highest bending strength (39 MPa) was measured with samples containing 25 wt.% monomer content and 50% solid loading. As the solid loading is decreased to 40, 30 and

20%, the bending strength is also decreased to 33, 29 and 21 MPa, respectively. The higher amount of the monomer content results in the increased polymer chain length and the bridging sites. The longer the polymer chain, the greater the numbers of entanglements that can form along

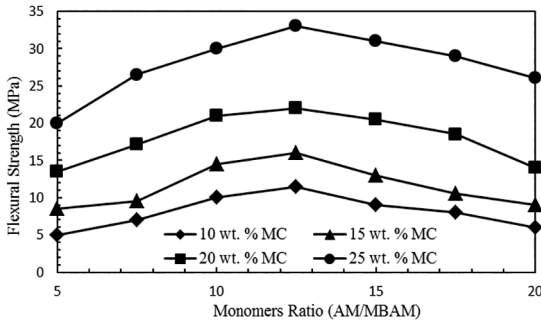


Figure 10: Dependence of the strength of green gelcast TiC on the monomer content as a function of monomer ratio for the 40 vol.% solid loading.

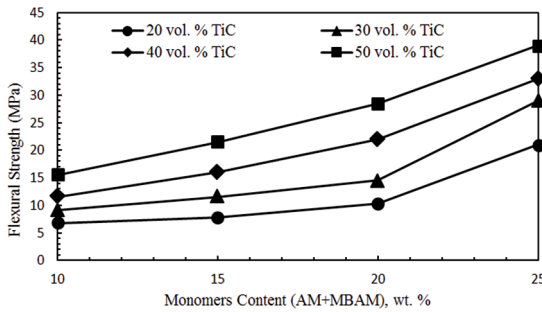


Figure 11: The bending stress of green gelcast TiC with varied solid loading as a function of monomer content.

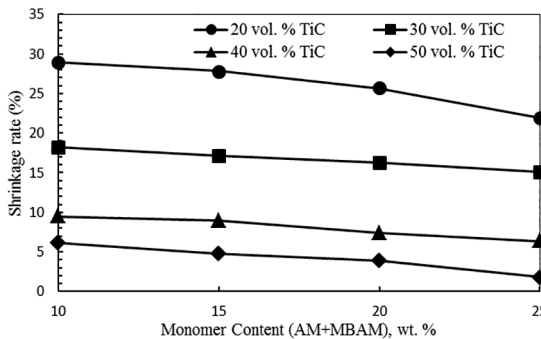


Figure 12: The influences of monomer content and solid loading on shrinkage rate of TiC green body.

it. Therefore, the longer the chain, the more difficult it is to distort the polymeric material. In addition to the linear macromolecules, polymer chains are often interconnected to form a nonlinear, branched, or crosslinked polymer. In the maximum value of the monomers content and solid loading, the three-dimensional network of the cross-linked polymer gels is compact and the cross-linked gel network adheres to the TiC particles and binds them together, providing the way for a uniform distribution of TiC powders in the green body²⁸.

Figure 12 shows the change of shrinkage rate as a function of monomer content and solid loading. Inspection of Figure 12 indicates that the lowest shrinkage rate of TiC green body was achieved with the highest monomer content and solid loading. The decrease could be attributed to the

strengthened 3D macromolecular network (as a result of the higher amount of the monomer content and solid loading), which helps to resist further contraction caused by the water evaporation. However, the higher solid loading means less inter-particle spacing and thus less water would be removed from the gel casted body resulting in smaller shrinkage which would occur during drying²⁸.

4. Conclusion

In this work, the effects of various parameters on the suspension rheology, gelation behavior and properties of titanium carbide green body were investigated. The dispersibility results proved that TMAH at 0.4 wt.% concentration can change the zeta potential of TiC suspension to -48 mV at the pH value 9. The influences of the monomer content, monomers ratio, initiator amount, ceramic solid loading and temperature were also evaluated by means of gelation time. The results showed that the increase in the monomer content, AM and MBAM concentration, initiator amount and temperature decreased the gelation time. It was found that the ceramic suspensions exhibit virtually an infinitesimal idle time compared to the pure monomer premixes.

The green strength TiC bodies prepared by gelcasting were shown to vary from ~ 5 MPa to over 39 MPa, depending on the solid loading, amount of monomers, and monomers ratio. The greatest strength was obtained with the gel casted samples containing 50 vol% solid loading, 25 wt.% monomers, and a monomer ratio of 12.5.

5. References

- Voitovich RF, Pugach EA. High-temperature oxidation of titanium carbide. *Soviet Powder Metallurgy and Metal Ceramics*. 1972;11(2):132-136.
- Dash R, Chmiola J, Yushin G, Gogotsi Y, Laudisio G, Singer J, et al. Titanium carbide derived nanoporous carbon for energy-related applications. *Carbon*. 2006;44(12):2489-2497.
- Kovalchenko MS. Pressure sintering kinetics of tungsten and titanium carbides. *International Journal of Refractory Metals and Hard Materials*. 2013;39:32-37.
- Cedat D, Libert M, Leflem M, Fandeur O, Rey C, Clavel M, et al. Experimental characterization and mechanical behaviour modelling of molybdenum-titanium carbide composite for high temperature applications. *International Journal of Refractory Metals and Hard Materials*. 2009;27(2):267-273.
- Gherrab M, Garnier V, Gavarini S, Millard-Ponard N, Cardinal S. Oxidation behavior of nano-scaled and micron-scaled TiC powders under air. *International Journal of Refractory Metals and Hard Materials*. 2013;41:590-596.
- Lin N, He Y, Wu C, Liu S, Xiao X, Jiang Y. Influence of TiC additions on the corrosion behaviour of WC-Co hardmetals in alkaline solution. *International Journal of Refractory Metals and Hard Materials*. 2014;46:52-57.

7. Osmęda A. Measurements of strain induced by chemical shrinkage in polymer composites. *Journal of Polymer Engineering*. 2016;36(4):431-440.
8. Yi ZZ, Xie ZP, Ma JT, Huang Y, Cheng YB. Study on gelcasting of silicon nitride-bonded silicon carbide refractories. *Materials Letters*. 2002;56(6):895-900.
9. Bandyopadhyay A, Bhowmick AK. Factors Influencing the Structure and Properties of Nanocomposites Derived by Sol-Gel Technique. *Journal of Polymer Engineering*. 2006;26(8-9):821-852.
10. Omatete OO, Janney MA, Strehlow RA. Gelcasting: a new ceramic forming process. *American Ceramic Society Bulletin*. 1991;70(10):1641-1649.
11. Motta O, Mamo A, Recca A, Aciemo D. Rheological and Calorimetric Characterization of an Epoxy System Cured in Presence of a Reactive Polyethersulphone. *Journal of Polymer Engineering*. 2000;20(3):159-174.
12. Jiang D. Gelcasting of carbide ceramics. *Journal of the Ceramic Society of Japan*. 2008;116(6):694-699.
13. Jiang DL. Gelcasting of carbide ceramics. *Key Engineering Materials*. 2009;403:163-164.
14. Foratirad H, Baharvandi HR, Maragheh MG. Effects of dispersants on dispersibility of titanium carbide aqueous suspension. *International Journal of Refractory Metals and Hard Materials*. 2016;56:96-103.
15. Paul A, Dobson D, James A. Infrared Spectroscopy of the TiO₂/Aqueous Solution Interface. *Langmuir*. 1999;15(7):2402-2408.
16. Zhang JX, Jiang DL, Tan SH, Gui LH, Ruan ML. Aqueous Processing of Titanium Carbide Green Sheets. *Journal of the American Ceramic Society*. 2001;84(11):2537-2541.
17. Zhang Q, Li W, Gu M, Jin Y. Dispersion and rheological properties of concentrated silicon aqueous suspension. *Powder Technology*. 2006;161(2):130-134.
18. Huang Q, Chen P, Gu M, Jin Y, Sun K. Effect of surface modification on the rheological behavior of concentrated, aqueous SiC suspensions. *Materials Letters*. 2002;56(4):546-553.
19. Bergström L. Shear thinning and shear thickening of concentrated ceramic suspensions. *Colloids and Surfaces A: Physicochemical and Engineering Aspects*. 1998;133(1-2):151-155.
20. Orbán M, Kurin-Csörgei K, Anatol M, Zhabotinsky AM, Epstein IR. Pattern formation during polymerization of acrylamide in the presence of sulfide ions. *The Journal of Physical Chemistry B*. 1999;103(1):36-40.
21. Morissette SL, Lewis JA. Chemorheology of Aqueous-Based Alumina-Poly(vinyl alcohol) Gelcasting Suspensions. *Journal of the American Ceramic Society*. 1999;82(3):521-528.
22. Babaluo AA, Kokabi M, Barati A. Chemorheology of alumina-aqueous acrylamide gelcasting systems. *Journal of the European Ceramic Society*. 2004;24(4):635-644.
23. Pethrick RA, Ballada A, Zaikov GE, eds. *Handbook of Polymer Research: Monomers, Oligomers, Polymers and Composites*. Hauppauge: Nova Science Publisher; 2007. 459 p.
24. Winter HH, Mours M. Advances in Polymer Science: Rheology of Polymers Near Liquid-Solid Transitions. In: *Neutron Spin Echo Spectroscopy Viscoelasticity Rheology*. Berlin, Heidelberg: Springer; 1997. p. 165-234.
25. Matyjaszewski K, Davis P. *Handbook of Radical Polymerization*. Hoboken: John Wiley & Sons; 2002.
26. Kriss M, ed. *Handbook of Digital Imaging*. Hoboken: John Wiley & Sons; 2015. 1824 p.
27. Yu J, Wang H, Zhang J, Zhang D, Yan Y. Gelcasting preparation of porous silicon nitride ceramics by adjusting the content of monomers. *Journal of Sol-Gel Science and Technology*. 2010;53(3):515-523.
28. Yu J, Wang H, Zeng H, Zhang J. Effect of monomer content on physical properties of silicon nitride ceramic green body prepared by gelcasting. *Ceramics International*. 2009;35(3):1039-1044.